Published in AJSE, Vol: 25, Issue:2
Received on 2nd June 2026
Revised on 16th September 2026
Published on 31st October 2026

AIUB JOURNAL OF SCIENCE AND ENGINEERING
ISSN: 1608 - 3679 (print) 2520 - 4890 (Online)
https://doi.org/10.53799/e1n87n43

QI-ResAFNet: Deep Learning Architecture for Intelligent Fault Diagnosis in Integrated Power Transmission System

Sanepalle Gopal Reddy[1*], Athimamula Srujana[2], Narender Reddy Narra[3], K. Shashidhar Reddy[4]

***Abstract*—The integration of energy sources into modern power transmission networks generated new challenges for accurate and adaptive fault diagnoses due to increased operational uncertainty, nonlinear disturbances, and varying data values. This study proposes a novel hybrid intelligent diagnostic architecture using a Quantum-Infused Residual Attention Fusion Network (Qi-ResAFNet) for high classification accuracy across various operational grid environments. Prior to extracting features, a systematic preprocessing of raw transmission-level dataset is performed including data cleansing, evaluation of data quality, and normalization prior to carrying out feature creation process. A comprehensive Exploratory Data Analysis (EDA) is then conducted to determine statistical characteristics, evaluate fault vs non-fault physical separation, and establish correlation patterns among the datasets. The feature engineering process is employed to create distinctive attributes from electrical signals in both time and frequency domains, thus providing improved representation of the signals for classification. The proposed Qi-ResAFNet is a new combination of quantum feature encoding, dual-attention fusion and deep residual network design to capture complex spatiotemporal correlations and quantum-enhanced interactions among features. The automated hyperparameter adjustment of the Heron Optimization Algorithm (HOA) significantly improve the generalization and convergence performance of the proposed architecture. Based upon the results produced by Python simulations of many fault-types under fluctuating energy supply, the proposed architecture achieves the highest accuracy, precision, recall and F1-Score of 0.99. This demonstrates that the proposed architecture provide rapid, reliable and flexible diagnostic capabilities of future intelligent transmission grids.**

***Keywords*—Preprocessing, Exploratory Data Analysis, Feature engineering, Quantum-Infused Residual Attention Fusion Network, Heron Optimization Algorithm.**

I. Introduction

RELIABLE transmission lines are the most important components in power transmission networks and their continued reliability provide stability and efficiency for the electrical power grid [1]. Faults in transmission lines, including short-circuits, open-circuits and insulation failures create large power outages, damage to equipment and the disruption of services. As a result the development of advanced fault detection is critical in limiting the potential effects of these failures and providing continued reliability to power systems [2-3].

Transmission networks have different types of faults, causing total or partial disconnections from the transmission network. Consequently, fast and precise analysis of transmission line faults and their locations is vitally important in order to prevent cascading failures leading to blackouts, in order to assure safe and continuous transfer of bulk electrical energy over long distances [4-6]. Permanent faults occur as a consequence of heating from excessive heat, deterioration of insulation or tearing caused by sudden load transfers or switch operations or tearing of the line due to natural disasters. Once a permanent fault is identified, the fault must be classified and located so that maintenance occur quickly [7-9]. Traditionally, fault location is accomplished by means of manual inspection techniques or by means of model-based techniques, including impedances and travelling waves. Initially, fault location methods based on impedance are used to determine where the failure occurred in a power system [10-11].

The impedance-based fault location methods require mathematical modeling, knowledge in the respective domain, a great deal of time, and many assumptions in order to function properly, therefore, their usefulness and dependability have diminished over time and are considered inadequate for today's modern power systems [12-14]. Unlike impedance-based methods, fault location methods based on travel time for a wave do not require mathematical models. However, they require the person operating to install expensive equipment at either end of a transmission line, and they cannot used on lines that have taps, such as three terminal lines or those with additional loads or sources [15].

Transmission line failures exhibit nonlinear and complex behaviours, with the primary difficulty in detecting faults attributed to the sheer volume of data produced by sensors located along the transmission line. Conventional methods for detecting faults through traditional means tend to work in some cases [16]. However, they usually do not perform in relation to dynamic or large-scale systems on both accounts, systems that produce an important amount of noise. In addition, the

Sanepalle Gopal Reddy was with Associate Professor, Department of Electrical and Electronics Engineering, Jyothishmathi Institute of Technology and Science, Karimnagar, Telangana. (sanepalle.gopal1980@gmail.com)
Athimamula Srujana was with Principal and Professor, Department of Electrical and Electronics Engineering, Vidya Jyothi Institute of Technology (VJIT), Hyderabad, Telangana. (srujanaa@yahoo.com)
Narender Reddy Narra was with Associate Professor in FDE, Military College of Electronics and Mechanical Engineering, Secunderabad, Telangana. (nnrrin84@gmail.com)
K. Shashidhar Reddy was with Professor, Department of Electrical and Electronics Engineering, CVR College of Engineering, Mangalpally, Ibrahimpatnam, R.R Dist. (shashidhar.kotha5@gmail.com)
*Corresponding author: Sanepalle Gopal Reddy

complexity of power transmission systems includes multiple interconnected parts and changes in environmental conditions, which greatly contributes to the overall complexity of diagnosing faults in power transmission systems. There has been a significant in using Deep Learning (DL) methods to solve difficulties faced with diagnosing faults in power transmission systems. With the ability of DL models to extract complex patterns from large datasets, it is applied very effectively to the diagnosis of faults in power transmission lines [17-19].

Furthermore, DL models have the capacity to acquire pertinent features from raw data automatically, eliminating the need for time-consuming, human generated, and error-prone feature extraction by using conventional methods [20]. Hence, the proposed system uses a hybrid intelligent diagnostic architecture using Qi-ResAFNet for intelligent fault diagnosis in integrated power transmission system. **Peichuan Sun *et al* [2023] [21]** have proposed a fault diagnosis in integrated power transmission system using Support Vector Machine (SVM). The SVM approach provides an effective method to identify non-linear fault patterns using kernel functions and allows for the reliable detection of complex transmission line fault types, including single line-to-ground, line-to-line and three phase faults. Additionally, it decreases the potential for overfitting by maximizing the margin of separation between classes thereby enhancing the overall generalization performance in a real-time monitoring environment. However, the training time and memory requirements increase dramatically with large scale power system data and massive amounts of real-time data. **Cheng Li *et al* [2023] [22]** have developed a power system fault diagnosis and classification using Random Forest (RF). In large-volume data sets with extensive numbers of dimensions, RF provide an effective methodology for dealing with complicated signals that are typically present in power systems such as voltage, current, and frequency. In addition, RF handle nonlinear relationships and noisy data, both of which are often got in real-time transmission environments. Though, it require additional computations, resulting in additional memory usage and prolonged processing time when utilizing in real time. **Nisreen Khalil Abed *et al* [2023] [23]** have suggested a K-Nearest Neighbours (KNN) method for detecting faults in power transmission line based on voltage and current. KNN is simple to implement and it is easy to deploy quickly. KNN performs for multiple classes of faults such as line-to-ground, line-to-line, and three-phase faults by comparing the current measurement or observation of the fault to historical recorded data from other faults. Nevertheless, the performance of KNN is negatively impacted if the training data contains a lot of noise, or if the selected features do not accurately represent the fault conditions and it have limitations in its ability to scale with large transmission systems. **Hassan N. Noura *et al* [2025] [24]** have established a fault detection and diagnosis in power transmission lines using Decision Tree (DT). DT are very effective at classifying both numerical inputs like voltage, current signals and categorical types of faults. DT requires very little computational power to classify the fault and is fast allowing for use in real-time protection type of applications. Additionally, DT automatically select the best features by selecting the variables in building the tree. Despite the ease of implementation and transparency using DT for diagnosing power transmission faults, DT is not generalize to highly non-linear and complex faults within the transmission system when compared to ensemble methods. **Rab Nawaz *et al* [2025] [25]** have proposed a Gradient Boosting method for integrated fault diagnosis in power transmission lines. This method is extremely virtuous for detecting nonlinear and complex faults in signals such as voltage and current. Gradient Boosting performs with mixed types of features and model complex relationships between the parameters of transmission systems. Moreover, Gradient Boosting gives the ability to evaluate feature importance, which aid in finding features that are important in detecting and classifying faults. Nonetheless, the time required to create training sets on large-scale datasets related to power transmission delay its use in real-time protection systems. The existing limitations of an integrated power transmission system is addressed using a hybrid fault detection system, Qi-ResAFNet. This system employs both residual learning and attention mechanisms to improve feature extraction and improve accuracy in classification. Additionally, the HOA is used to perform hyperparameter tuning to ensure that the model reaches optimal configuration, converges quickly, and enhanced diagnostic reliability.

A. Objectives:

The primary objectives of this study comprises,

- To produce statistical summaries, examine correlations, and investigate distribution patterns in order to identify variations between fault and non-fault circumstances, EDA is implemented.
- To improve the model's discrimination capabilities and reflect system dynamics, feature engineering is executed.
- To enhance accurate classification and robustness of system states, Qi-ResAFNet utilized.
- To increase convergence speed, stability, and overall classification performance, the Heron Optimization Algorithm is used to tune model hyperparameter.

II. Proposed System Description

The proposed method provides a detailed and advanced analysis for fault detection within an integrated electric power delivery system through a hybrid Qi-ResAFNet. The block diagram of Qi-ResAFNet classification is displayed in Fig. 1.

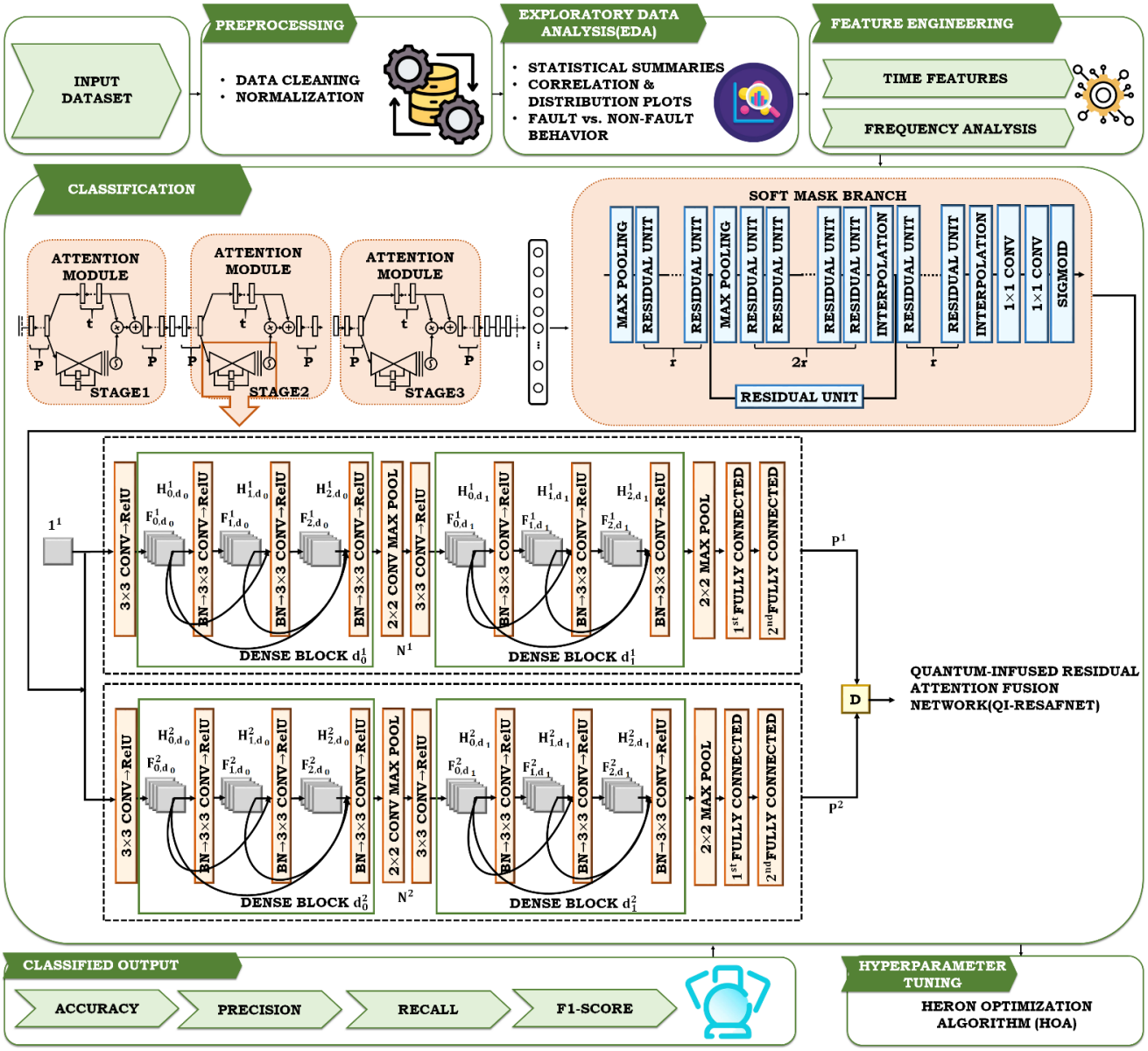

Fig. 1. Proposed block diagram.

The process begins by performing preprocessing the raw data set by cleaning and normalizing the data to eliminate inconsistencies and noise, and create an equivalent representation of the data. After preprocessing, EDA is performed to determine the statistical properties of the data, correlation between variables, and distribution of the observed values to enhanced both fault and non-fault characteristics. Discriminative features in both the time and frequency domains is derived in the feature engineering stage, which provide both temporal dynamics and frequency information of the signals transmitted by the system, thus enhancing the ability to distinguish between normal and faulty system operation. The Qi-ResAFNet classifier receives enriched features, and its deep feature propagation through the use of residual learning reduces gradient vanishing. An attention mechanism prioritizes the use of informative features. The hybrid classifier improves the representation of features, facilitates more efficient learning process and more reliable classification results. In addition, the evaluation of fault and non-fault conditions is enhanced through hyperparameter tuning with the HOA. The advantages of using HOA are optimal parameters, quicker convergence of the model, and improved generalization. The final output of the classification system provides an accurate evaluation of fault and non-fault conditions and assist in providing reliable, robust, and effective diagnosis of faults, depending on actual operating conditions.

III. Proposed System Modelling

A. Preprocessing:

Preprocessing is an important step to ensure the intelligent fault diagnosis of electricity transmission systems accurately and reliably. The purpose of this stage is to provide the data generated by voltage, current, frequency, and other types of sensor signals to advanced computational models for effective fault detection and classification.

1) Data Cleaning:

Data cleaning is a significant role in applying intelligent fault diagnosis for integrated power transmission systems as they consist of many different components across multiple locations providing heterogeneous data. It is used to accommodate the wide variability in operational conditions and signals. This generally involves structured operations such as collecting data from the system, assessing the mechanical or electrical systems that generate the data and identifying noise within a particular measurement due to disturbances. Once the inconsistencies or invalid measurements are removed from the dataset, more valid data points are provided for subsequent processing of the data and the dataset is given as a compiled CSV file.

2) Normalization:

Intelligent fault diagnosis for integrated power transmission systems uses various monitoring devices of networks from multiple locations which include electrical and operating data such as voltage, current, frequency, power, impedance, temperature, and vibration within each substation and transmission element. Due to different voltage levels and equipment ratings, these measurements frequently have large numbers with different numerical ranges. To create a uniform scale for this data, each parameter is equally weighed, the normal process is to apply Min-Max normalization to rescale all of the parameters, typically in a range of [0, 1]. The normalized value of a measurement using Min-Max normalization is calculated as,

$$X_{Scaled} = \frac{X - X_{min}}{X_{max} - X_{min}} \quad (1)$$

Where, X_{Scaled} characterizing the original measured value, X_{min} and X_{max} are the respective min and max values for the characterizing parameter.

The primary benefits associated with the use of min-max normalization in integrated power transmission systems include, low computational complexity and applicable to real-time monitoring environments. Therefore, the intelligent fault detection system provide a timely response and more accurately detect anomalous conditions within the transmission system.

B. Exploratory Data Analysis

1) Statistical Summaries:

The use of statistical summaries is important for intelligent fault diagnosis in analyzing electrical parameters like voltage, current, frequency, and power through the calculation of means, standard deviations, variances, distributions. By analyzing these metrics, deviations from normal operational states are identified, revealing abnormalities such as sudden flows in current, drops in voltage, or fluctuations in either measurement, which typically indicates faults within transmission lines.

2) Correlation and distribution plots:

Analyzing correlations helps to identify connections between multi-phase voltage and current signals during fault events by determining interdependency among those associated with particular phases. Distribution plots show the behaviour of data under both normal and faulty conditions, therefore the distribution of values for faulty parameters typically have skewed distributions and differentiated from the normal behaviour of the system.

3) Fault vs Non-Fault behavior:

When differentiating between healthy and unhealthy operating states, EDA provides insight into each variable behaves under different operating conditions and therefore supports accurate feature selection for improved performance, reliability, and accuracy of intelligent fault classification models used to monitor and manage integrated power transmission systems.

C. Feature Engineering:

Feature engineering is the most important processes of identifying faults through a high level of intelligence using voltage and current signals from transmission lines to create individual values that significantly enhance the quality of the classification systems.

TABLE I
FEATURE SUMMARY FOR THE PROPOSED Qi-ResAFNet

Attribute	Description
Input features	Ia, Ib, Ic, Va, Vb, Vc
Feature extraction	Time domain and frequency domain
Feature scaling	Standard scalar
Feature selection	Not applied
Dimensionality reduction	Not applied

The feature engineering phase involves generating data from the electrical signals, namely Ia, Ib, Ic, Va, Vb, and Vc. From the time and frequency dimensions of these signals, time-domain and frequency-domain features are generated to provide reliable information about fault occurrences. The generated features are passed to the Qi-ResAFNet classifier to compute the outcome.

1) Time features:

Time-domain features are extracted from electrical signals that captured in their original state. They include cumulative movement over time, maximum and minimum values, average, amount of scattered data, magnitude of dispersion, degree of error from the mean, frequency of very large or small events, ratio of the largest signal's amplitude to the average amplitude and overall amount of signal energy. Time-domain features capture these abrupt changes very effectively and help to determine the faults such as current, voltage and wave forms associated with the system, because these features, it is ideal for monitoring and protecting against faults in real-time.

2) Frequency analysis:

Frequency domain analysis are conducted by transforming time-based signals into frequency terms. Harmonics, sub-harmonics, and complicating frequency behavior result from the switching of transmission lines, insulation failures, and electrical arcing faults. To characterize the type of fault

occurring in the transmission lines, the types of faults include the use of dominant frequency components, bandwidth across the entire frequency spectrum and the cumulative effect of harmonic distortion. Also, frequency-domain features is beneficial when differentiating between transient and sustained fault events, and identifying issues associated with the power quality of the energy supply.

D. Classification - Quantum-Infused Residual Attention Fusion Network:

The diagnostic transformation using a reconstructed process matrix (X_{expt}) that maps the various multi-sensor measurements such as voltage, current, frequency, harmonics, temperature, and vibration for making fault decisions. The model contains quantum enhancements beyond classical approaches, the key characterization are summarized below. The quantum compositionality definition defines the smallest amount of a true quantum component that is found in the diagnostic transformation,

$$X_{expt} = \alpha X_Q + (1-\alpha)X_C \tag{2}$$

Where, X_Q denotes the quantum parts, X_C represents the classical aspects, α is a minimal amount of quantum and a non-zero value for α verifies that the quantum-infused model includes inherent quantum correlations between the signals of the transmission system and do not contain classical feature extraction. In terms of noise and other types of disturbances, the process robustness measures the quantum-infused model.

$$\frac{X_{expt}+\beta X'}{1+\beta} = X_C \tag{3}$$

In the framework for defining noise, β represents the minimal amount of noise required to convert a quantum process into a classical process, higher values denote greater robustness of the diagnostic framework to measure uncertainties and system perturbations. The fidelity condition provides a means to assess the degree of similarity between the process implemented and the ideal target quantum fault classifier $\chi\ Q\ T$ (chi QT).

$$F_{expt} \equiv tr\left(X_{expt}\ X_{Q_T}\right) > F_C \equiv \max_{X_C} tr\left(X_C X_{Q_T}\right) \tag{4}$$

If this inequality holds, then the quantum-infused approach provides a significant improvement in diagnostic ability over the best classical model. Finally, the entropy measure provides to evaluate the information structure of the diagnostic transformation.

$$S\left(X_{expt}\right) < S_C \equiv \min_{X_C} S(X_C) \tag{5}$$

Lower entropy indicates structured quantum correlations and lower uncertainty in fault classification. This provide a quantum contribution, robustness and enhanced diagnostic capability of the quantum-infused intelligent fault diagnosis framework for integrated power transmission systems.

The Qi-ResAFNet mentioned is merely inspired by quantum technology in its proposed design and hence does not involve the use of quantum hardware, quantum circuits, quantum operations, or phenomena like entanglement or superposition. The quantum process matrix, fidelity, and entropy equations as formulated are simply employed to represent the interactions of features in addition to the uncertainty and relationships of information in the diagnostic process. Such formulations give a theoretical upgrade to the feature representation but use classical DL technology throughout the overall approach.

Residual Attention is used to extract and refine electrical characteristics through measurements of multiple sensors, such as voltage, current measurement, frequency deviation or harmonic distortion. Let the multi-channel input signal is denoted by the element $\epsilon R^{C\times T}$. Each attention module has a trunk branch, which extracts nonlinear deep features, producing feature maps$T(x)$, representing fault-sensitive attributes such as signal transients, oscillatory signals, and distorted waveforms due to interaction with the grid, and a mask branch which has a bottom up or top down hierarchy to generate an attention map $M(x)$ that is the same as $T(x)$ but is used for hierarchical modeling of local disturbances and anomalies at a system-wide level. After the attention module processes the output signal is as follows,

$$H_{i,c}(x) = M_{i,c}(x) * T_{i,c}(x) \tag{6}$$

The temporal position is given by i and the index of the channel used for transmission is given by $c \in \{1, 2\ldots\ C\}$. The mask value $M_{i,c}(x) \in [0, 1]$ provides adaptive control gates that allow the model to emphasize the important fault-related features, while reducing the impact of measurement noise. When the model is being trained using back propagation, the trunk branch parameter gradient is modulated using the learned mask parameters by the following equation,

$$\frac{\partial M(x,\theta)T(x,\phi)}{\partial \phi} = M(x,\theta)\frac{\partial T(x,\phi)}{\partial \phi} \tag{7}$$

The gradient filtering process eliminates the impact of irrelevant or noisy components on the parameters updates, which improves robustness to mislabelled examples of faults that contain ambiguity. Multiple attention modules stack together to progressively refine features across the various networks layers, model waveform-level disturbances, intermediate networks, model harmonic, frequency-related disturbances and deep networks, classify at the fault-level. Thus, the residual attention provides multi-scale learning, which is resilient to noise, and provides equitable learning for intelligent fault diagnosis on integrated power transmission systems. The structure of Qi-ResAFNet is shown in Fig. 2.

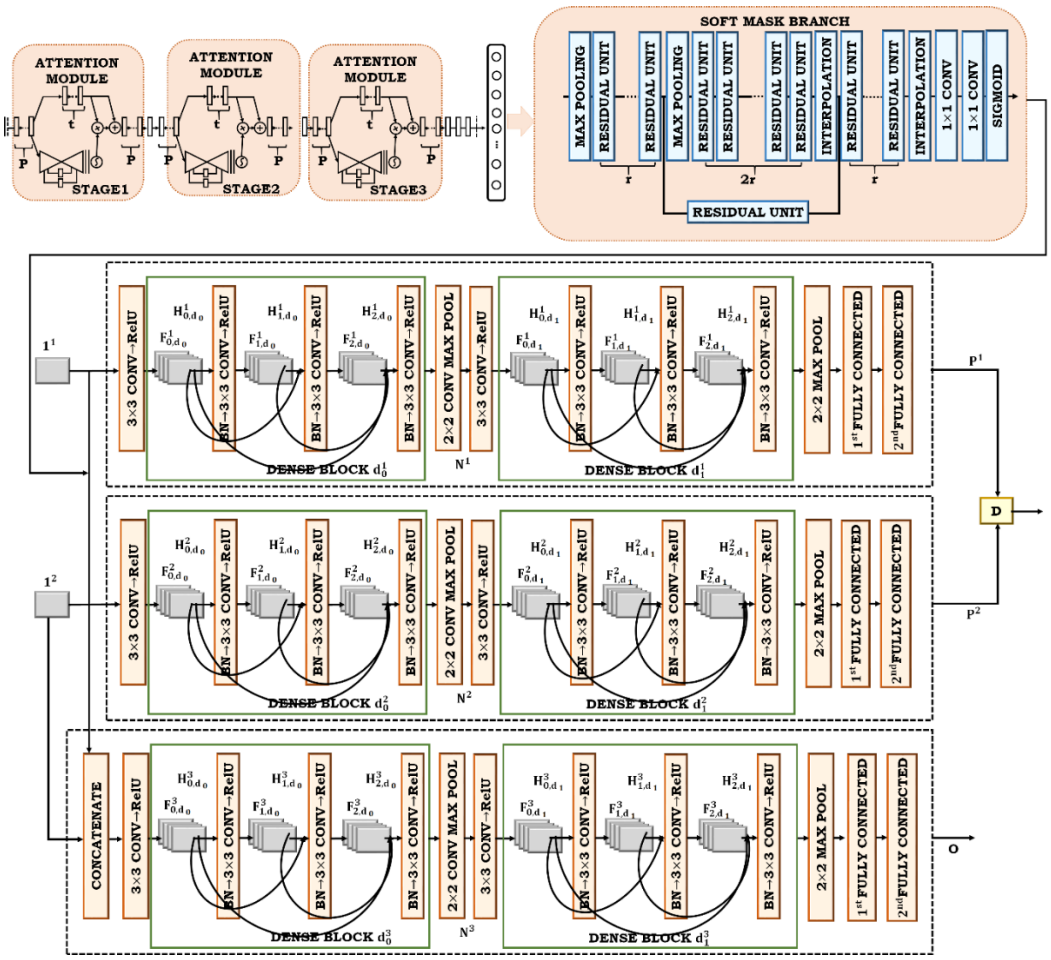

Fig. 2. QI-ResAFNet model.

When diagnosing faults in integrated power transmission systems, the analysis is made based on two temporal operating states, the reference state S_1 (normal condition) and the current state S_2 (suspected faulty condition). Measurement abnormalities for voltage, current, frequency, phase angle, and power flow are detected by comparing these states directly. However, direct comparisons of low-level electrical features are susceptible to measurement noise, synchronization errors, switching disturbances, and load changes, which produce a false alarm. Using high-level abstract representations possibly will not detect the incipient faults. To resolve this issue and achieve a detection mechanism that is balanced and reliable, a three-branch (N_1, N_2, N_3) dense convolutional fusion architecture is utilized. The purpose of the first and second branches is to extract feature sets from the two temporal operating states S_1 andS_2. The third branch of the architecture uses the concatenated representations from the first two branches to acquire correlated fault characteristics. By creating a densely connected representation, the architecture creates an invariant representation of the fault by reusing feature maps from all preceding layers. The feature maps of the l^{th} layer from the r^{th} dense block of the i^{th} branch are computed as follows,

$$F^i_{l,dr} = H^i_{l-1,dr}\left(\left[F^i_{0,dr}, F^i_{1,dr}, \ldots F^i_{l-1,dr}\right]\right), r = 0,1; i = 1,2,3 \quad (8)$$

The concatenation of all previous feature maps is represented as $[\cdot]$, while $H(\cdot)$ is a composite of batch normalization, 3 x 3 convolution and ReLU activation functions is applied. Using the dense formulation extracts features allows for additional propagation of features, increases the flow of gradients and improves the ability to learn invariant transit fault signatures. Once features are extracted from both N_1 and N_2 , they are passed through a sigmoid activation function to yield embeddings P^1 and P^2 then, the dissimilarity of the two operational states is calculated based on the Euclidean distance,

$$D = \| P^1 - P^2 \|_2 \quad (9)$$

Where, D indicates more significant difference between normal functioning and current grid conditions. Two concatenated inputs $[S_1,S_2]$ are used to determine an output O that indicates the probability of a fault in the current state as expressed by $O \in [0,1]$. The two outputs, D and$O$ provide two types of complementary diagnostic information. D provides the extent of the deviation from normal grid condition, O provides the probability of a fault occurring. Using both combined outputs, reduces the potential for incorrect identification of a fault by minimizing both false positives and false negatives.

The Qi-ResAFNet offers an intelligent means for diagnosing faults in integrated power transmission. The quantum element improves diagnosis by providing a structured relationship

between features to enhance diagnostic capability, increase robustness to noise, and reduce uncertainty. The use of the residual attention mechanism highlights features associated with faults while reducing noise to facilitate multi-scale and resilient feature learning. The fusion architecture improves reliability even further by determining the normal state and fault state for each feature's probability of fault and deviation magnitude. This framework provides an accurate, noise-tolerant, and reliable diagnosis of faults in dynamic power systems.

E. Optimization- Heron Optimization Algorithm:

The HOA method is designed to further enhance the Qi-ResAFNet for intelligent diagnosis of faults in integrated power transmission systems. This method is used to optimally set the parameters desired to diagnose faults like feature weights, classifier coefficients, decision thresholds and deep learning hyperparameter from multi-sensor data including voltage, current, frequency deviation, harmonic distortion, temperature and vibration signals. Each heron's position represents a potential solution vector of diagnostic parameters X_i and evaluated to determine a ranking for each solution using a fitness function $f(X_i)$ which measures classification accuracy, fault detection rate or error minimization.

During the camouflage-predation phase of the algorithm, a density-based local search is performed around the current solution. To perform this method, the density of local neighbours are first calculated to estimate many neighbours exist in the surrounding search area. When the density is high, there are a lot of neighbours with similar set of diagnostic parameters. Where the stagnation occurs around the current neighbourhood solution which cause the search to stuck at a local optimum.

$$D_i = \sum_{j=1}^{k} \frac{1}{1+\|X_j - X_i\|} \tag{10}$$

Following that, the locality of the search is defined based on comparing the fitness of neighbouring solutions to define a direction of search towards a diagnostic configuration with an improved fault discrimination capability. The gradient term define a direction in which candidates move toward potential diagnostic configurations with better performance than current ones.

$$G_i = \frac{\sum_{j=1}^{k}(X_j - X_i)\left(f(X_i) - f(X_j)\right)}{k} \tag{11}$$

Additionally, step size are modified for adaptive refinement according to computed density, small steps are taken for high density areas for fine tuning and large steps are made for low density areas to improve exploration.

$$Step_i = \frac{\delta}{1+D_i} \tag{12}$$

The result of this process is a new diagnostic parameter vector and is defined below,

$$X_i^{new} = X_i + Step_i \cdot normalize(G_i) \tag{13}$$

In order to hasten the convergence to the optimal diagnostic configuration, the neck retraction mechanism models a rapid approach towards the best solution. This mechanism serves to enhance the speed, where convergence is achieved during the early iterations of the search and progressively stabilizes an ongoing search in the later iterations of the search to avoid oscillations.

$$X_i^{new} = X_i + \gamma(X_{best} - X_i)\left(1 - \frac{t}{MaxIter}\right) \tag{14}$$

Where, X_{best} is the globally best diagnostic solution, γ is the acceleration factor, t is the current iteration number and $MaxIter$ is the maximum number of iterations.

To balance global exploration with local exploitation while diagnosing nonlinear and complex faults within an electrical power transmission system, a hierarchical foraging strategy is utilized. As the current iteration progresses, the probability of performing global exploration is reduced exponentially, allowing for greater opportunities for searching in the initial phase and more opportunities for refined exploitation in the final phase.

$$p_{global}(t) = exp\left(-\lambda \frac{t}{MaxIter}\right) \tag{15}$$

Here, λ is a parameter that determines quick global exploration which decay. The robustness of ecosystem-aware migration is based on its ability to withstand a variety of operations of the grid, including load changes, disturbances and uncertain data from sensors. The flowchart of HOA is depicted in Fig. 3.

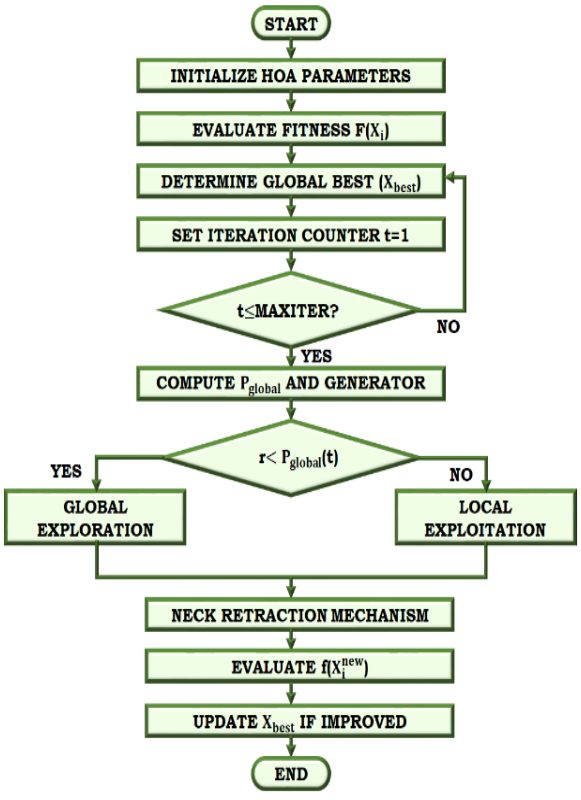

Fig. 3. Flowchart of HOA.

A measure to fit the environment for the individual is calculated using a value called a suitability function, $S(X)$. Each individual migrates to the most proximal environment, which provides it with the most suitable alternative.

$$X_{env_best} = \arg \max_{X_{neighbor}} S(X_{neighbor}) \quad (16)$$

$$X_i^{new} = X_i + \beta \cdot rand() \cdot (X_{env_best} - X_i) \quad (17)$$

Where, β is the migration step size, and $rand()$ represents a random perturbation. These processes helps to accelerate convergence rates, increase accuracy in fault classification, deter premature stagnation, and provide a robust and intelligent fault diagnostic capability within a connected power transmission system.

IV. Result And Discussion

The Qi-ResAFNet-HOA approach is tested with data collected from multi-sensor measurements taken from a power transmission integrated system under both normal and multiple fault conditions. Some of the variables in the dataset collected are voltage, current, frequency deviation, harmonic distortion, temperature and vibration.

TABLE II
DESCRIPTION OF DATASET

DATASET DESCRIPTION	
Dataset Name	Electrical fault detection and classification
Data Source	Kaggle
File Name	Classdata.csv
Train-Test split	80:20
Total Features	10
Features Name	G, C, B, A, Ia, Ib, Ic, Va, Vb, Vc
Input features (X_Labels)	'Ia', 'Ib', 'Ic', 'Va', 'Vb', 'Vc'
Output feature (Y Labels)	Create the Target Feature Using G,C,B,A
Y Labels	Fault_Type
Class names (Fault_Type)	LG Fault, LLG Fault, LLL Fault, No Fault, Other
Class	6
Total Counts	7861
Feature Count	11
Fault Type	No Fault - 2365 LLG Fault - 1134 LLLG Fault - 1133 LG Fault - 1129 LLL Fault - 1096 Other - 1004

Table II shows the description where electrical fault detection and classification dataset is used. It consists of 7861 records with 10 total features (G, C, B, A, Ia, Ib, Ic, Va, Vb, and Vc). Among these, six features (la, lb, lc, Va, Vb, Vc), are considered as inputs features and the output feature, Fault_Type is generated by combining G, C, B, and A. Six fault classes are considered in the dataset, namely No Fault, LG Fault, LLG Fault, LLLG Fault, LL Fault and Other. The initial data is split into 80% for training and 20% for testing purposes, which allowed to create a well-structured dataset for the purpose of developing and testing the fault classification model.

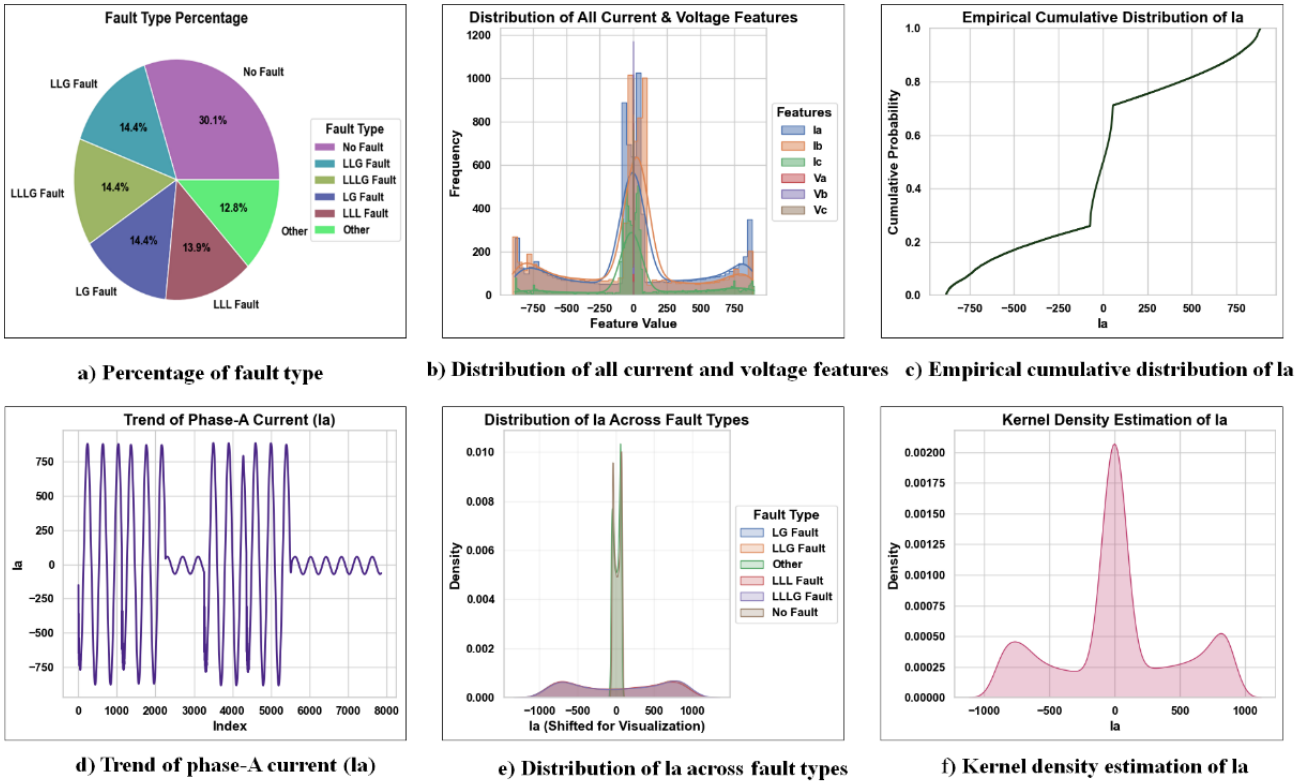

a) Percentage of fault type
b) Distribution of all current and voltage features
c) Empirical cumulative distribution of Ia
d) Trend of phase-A current (Ia)
e) Distribution of Ia across fault types
f) Kernel density estimation of Ia

Fig. 4. a) Percentage of fault type, b) Distribution of all current and voltage features, c) Empirical cumulative distribution of Ia, d) Trend of phase-A current (Ia), e) Distribution of Ia across fault types, f) Kernel density estimation of Ia.

Fig. 4 displays the distribution of fault types based on data and statistical evaluations of phase A (Ia) current. It indicates that the case with No Fault is at the highest percentage when compared to the other faults, with even distribution across the

remaining faults. The plots illustrate both the variation, cumulative behavior, trend over time, and the density of current (Ia) for different faults. There are many unique traits associating with various situations that relate to the existing faults.

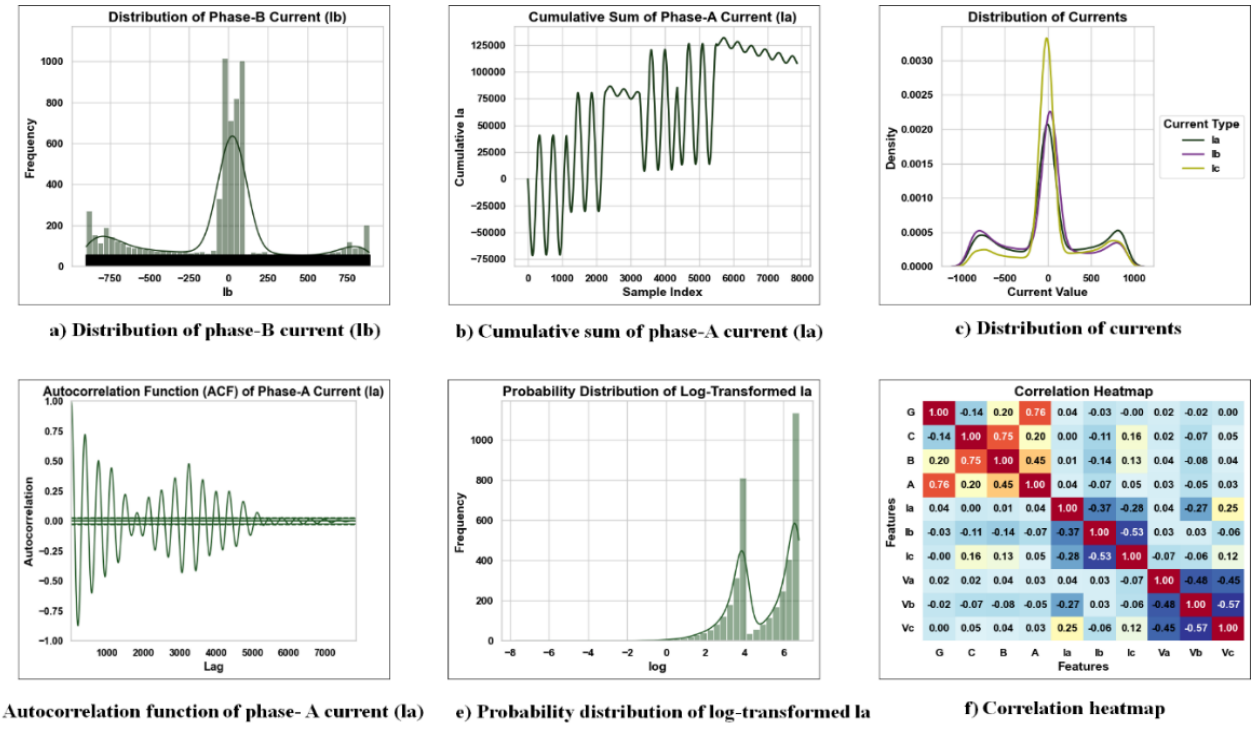

Fig. 5. a) Distribution of phase-B current (Ib), b) Cumulative sum of phase-A current (Ia), c) Distribution of currents, d) Autocorrelation function of phase- A current (Ia), e) Probability distribution of log-transformed Ia, f) Correlation heatmap.

Fig. 5 provides statistical evaluation of current signals in order to include the distribution of phase B (Ib) current, cumulative behavior of phase A (Ia) current, and a comparison of current density (Ia versus Ib and Ic). It also provides an autocorrelation of phase A (Ia) current and the log-transformed current distribution for phase A (Ia), along with a comparison matrix that illustrates the correlation between all current and voltage-related features.

TABLE III
CLASSIFICATION REPORT OF THE PROPOSED SYSTEM (QI-RESAFNET-HOA)

	ACCURACY	PRECISION	RECALL	F1-SCORE
LG Fault	0.99	1.00	1.00	1.00
LLG Fault	0.99	0.97	0.98	0.97
LLL Fault	0.99	0.98	0.96	0.97
LLLG Fault	0.99	1.00	1.00	1.00
No Fault	0.99	1.00	1.00	1.00
Other	0.99	1.00	1.00	1.00
Weighted Average	0.99	0.99	0.99	0.99

In table III, Qi-ResAFNet-HOA developed a model that achieved an accuracy greater than or equal to 99% with precision, recall and F1-scores near or equal to 0.99 for all fault categories. As such, most of the numerous fault categories produced a perfect or near perfect identification of the fault category type in this research, making the fault classification performance highly reliable and robust.

While the suggested model indicated high classification performance, it is important that the results should be examined in the characteristics of the dataset. The dataset is composed of distinct fault categories and their corresponding distinctive electrical features that make it easier to differentiate between them. Moreover, fivefold cross-validation is conducted to assess robust and generalizable, and the results through all the folds of the models are consistent with each other, supporting the accuracy of the results in this work.

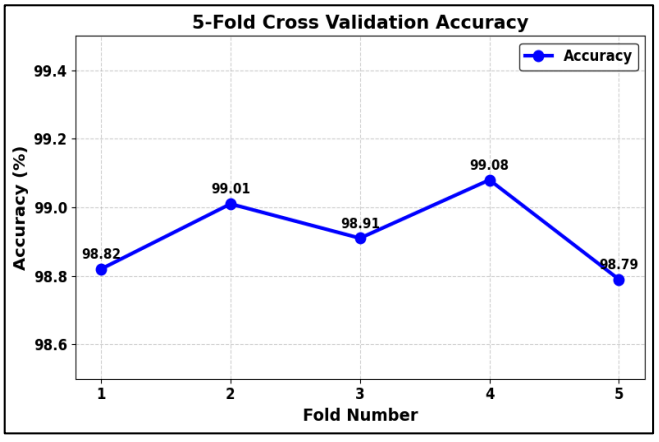

Fig. 6. 5-Fold cross validation accuracy

The 5-fold cross-validation accuracy is shown in Fig. 7. The model produces high accuracy, between 98.79% and 99.08%. Its best performance is in Fold 4 (99.08%) while the lowest accuracy is in Fold 5 (98.79%). The small variation of the model's performance across folds shows that it is consistent and reliable.

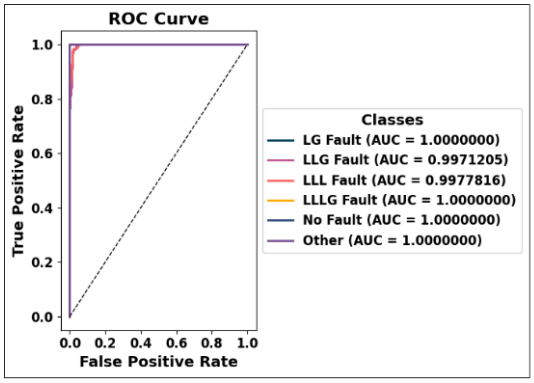

a) ROC curve for Qi-ResAFNet-HOA

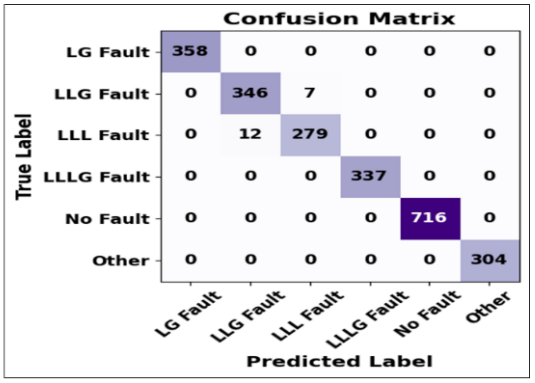

b) Confusion matrix for Qi-ResAFNet-HOA

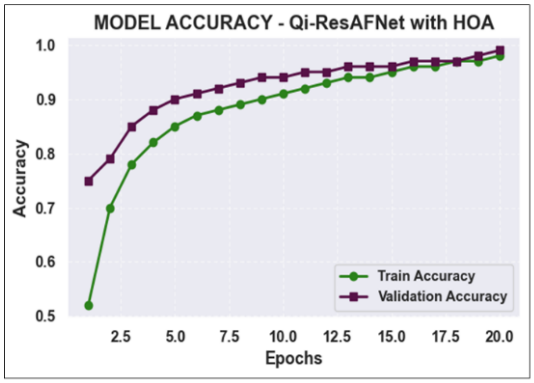

c) Model accuracy for Qi-ResAFNet-HOA

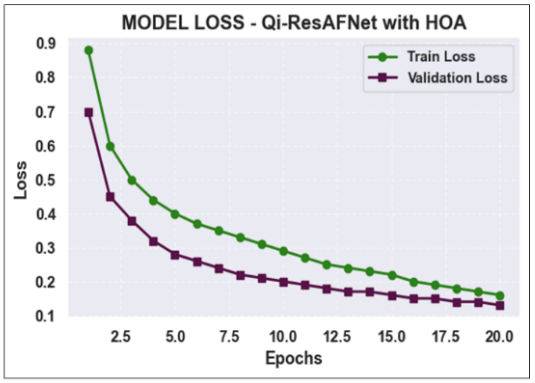

d) Model loss for Qi-ResAFNet-HOA

Fig. 7. a) ROC curve for Qi-ResAFNet-HOA, b) Confusion matrix for Qi-ResAFNet-HOA, c) Model accuracy for Qi-ResAFNet-HOA, d) Model loss for Qi-ResAFNet-HOA.

Fig. 7 indicate that Qi-ResAFNet-HOA achieved a perfect classification with the AUC values approaching 1.0 and few incorrect classifications being noted in the confusion matrix. The training and validation accuracy approaches approximately 99% with a continued steady decline in loss indicating stable convergence and thus producing a highly reliable model.

TABLE IV
CLASSIFICATION REPORT OF QI-RESAFNET

	ACCURACY	PRECISION	RECALL	F1-SCORE
LG Fault	0.96	1.00	1.00	1.00
LLG Fault	0.96	0.97	1.00	1.00
LLL Fault	0.96	0.92	0.70	0.80
LLLG Fault	0.96	0.81	0.95	0.87
No Fault	0.96	1.00	1.00	1.00
Other	0.96	1.00	1.00	1.00
Weighted Average	0.96	0.96	0.96	0.96

Qi-ResAFNet demonstrates an accuracy of approximately 96% with excellent results across most fault groupings in table IV. LLL and LLLG fault types, present notably lower recall and F1-scores. This limits the effectiveness of the entire model. Overall, the model shows strong classification across the board but is below that of the improved model.

In Fig. 8, Qi-ResAFNet achieves roughly 96% accuracy on the dataset with very high AUC for the majority of the fault types, however there is a large amount of misclassification between LLL and LLLG. Qi-ResAFNet continues to show stable training with steadily increasing accuracy and steadily decreasing loss. The enhanced version of Qi-ResAFNet performs at a higher level.

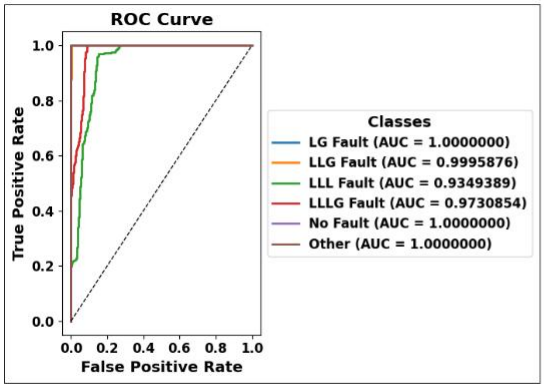

a) ROC curve for Qi-ResAFNet

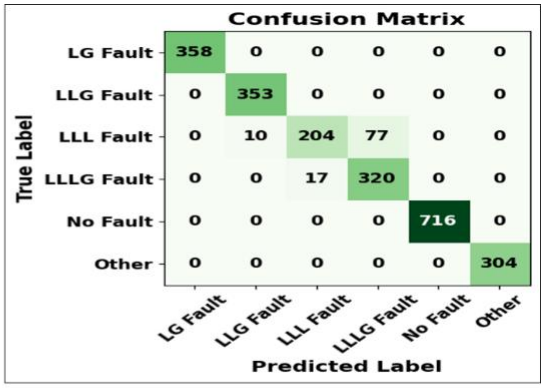

b) Confusion matrix for Qi-ResAFNet

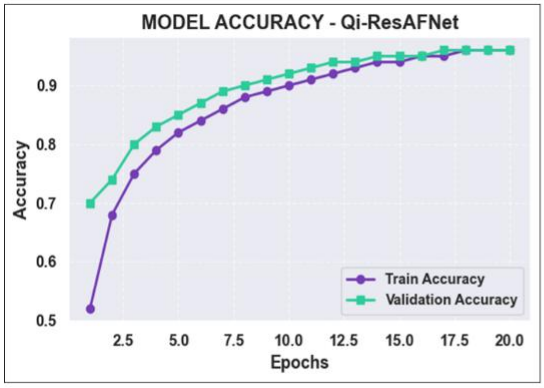

c) Model accuracy for Qi-ResAFNet

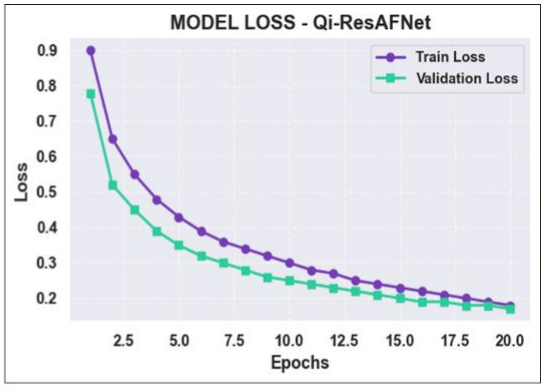

d) Model loss for Qi-ResAFNet

Fig. 8. a) ROC curve for Qi-ResAFNet, b) Confusion matrix for Qi-ResAFNet, c) Model accuracy for Qi-ResAFNet, d) Model loss for Qi-ResAFNet

TABLE V
CLASSIFICATION REPORT OF RESAFNET

	ACCURACY	PRECISION	RECALL	F1-SCORE
LG Fault	0.91	1.00	1.00	1.00
LLG Fault	0.91	0.98	0.90	0.94
LLL Fault	0.91	0.81	0.56	0.66
LLLG Fault	0.91	0.66	0.89	0.75
No Fault	0.91	1.00	1.00	1.00
Other	0.91	1.00	1.00	1.00
Weighted Average	0.91	0.91	0.91	0.91

In table V, ResAFNet has an accuracy of about 91%, and very good detection performance across the majority of all faults, whereas LLL and LLLG fault type detection ability is the other fault types resulting in lower recall and F1-scores. Therefore, overall, ResAFNet is not as effective as the enhanced models.

Fig. 9 results shows ResAFNet achieves approximately 91% accuracy on the entire dataset, with very high AUC for most fault types. A large number of incorrect classifications occurred between LLL and LLLG, indicating that the model exhibited unstable training across most artificial neural networks trained during this time period. The enhanced ResAFNet performs at a higher accuracy than the current model.

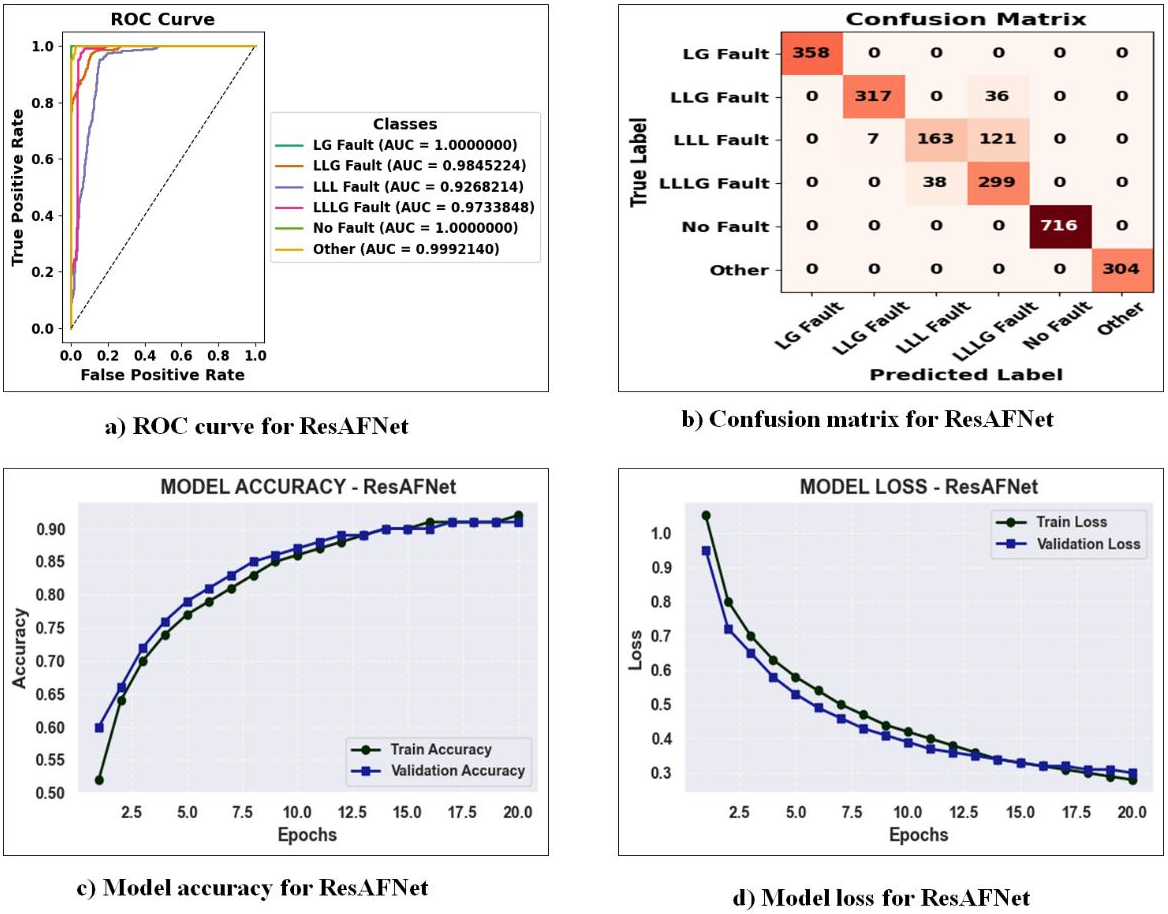

a) ROC curve for ResAFNet

b) Confusion matrix for ResAFNet

c) Model accuracy for ResAFNet

d) Model loss for ResAFNet

Fig. 9. a) ROC curve for ResAFNet, b) Confusion matrix for ResAFNet, c) Model accuracy for ResAFNet, d) Model loss for ResAFNet

TABLE VI
CLASSIFICATION REPORT OF AFNET

	ACCURACY	PRECISION	RECALL	F1-SCORE
LG Fault	0.90	1.00	0.76	0.87
LLG Fault	0.90	0.95	0.96	0.96
LLL Fault	0.90	1.00	0.87	0.93
LLLG Fault	0.90	0.91	1.00	0.95
No Fault	0.90	0.79	1.00	0.88
Other	0.90	1.00	0.64	0.78
Weighted Average	0.90	0.91	0.90	0.89

In table VI, the AFNet model provides an accuracy of about 90%, with some fault classes achieving high performance while others exhibit imbalanced precision versus recall scores. As a result, its overall classification performance is at moderate levels compared to enhanced classifiers.

TABLE VII

DATASET COUNT

Fault Type	Count	Percentage (%)
No Fault	2365	30.09
LLG Fault	1134	14.43
LLLG Fault	1133	14.41
LG Fault	1129	14.36
LLL Fault	1096	13.94
Other	1004	12.77
Total	7861	100.00

The dataset comprises 7,861 fault occurrences spread over six fault classifications in table VII. The No Fault class is the largest class containing 2,365 samples (30.09%), followed by the LLG fault (14.43%) class, the LLLG fault (14.41%) class, the LG fault (14.36%) class, and the LLL fault (13.94%) class. The other category consists of 1,004 samples (12.77%). In general, the fault classes are well-balanced apart from having a larger percent of the No Fault class.

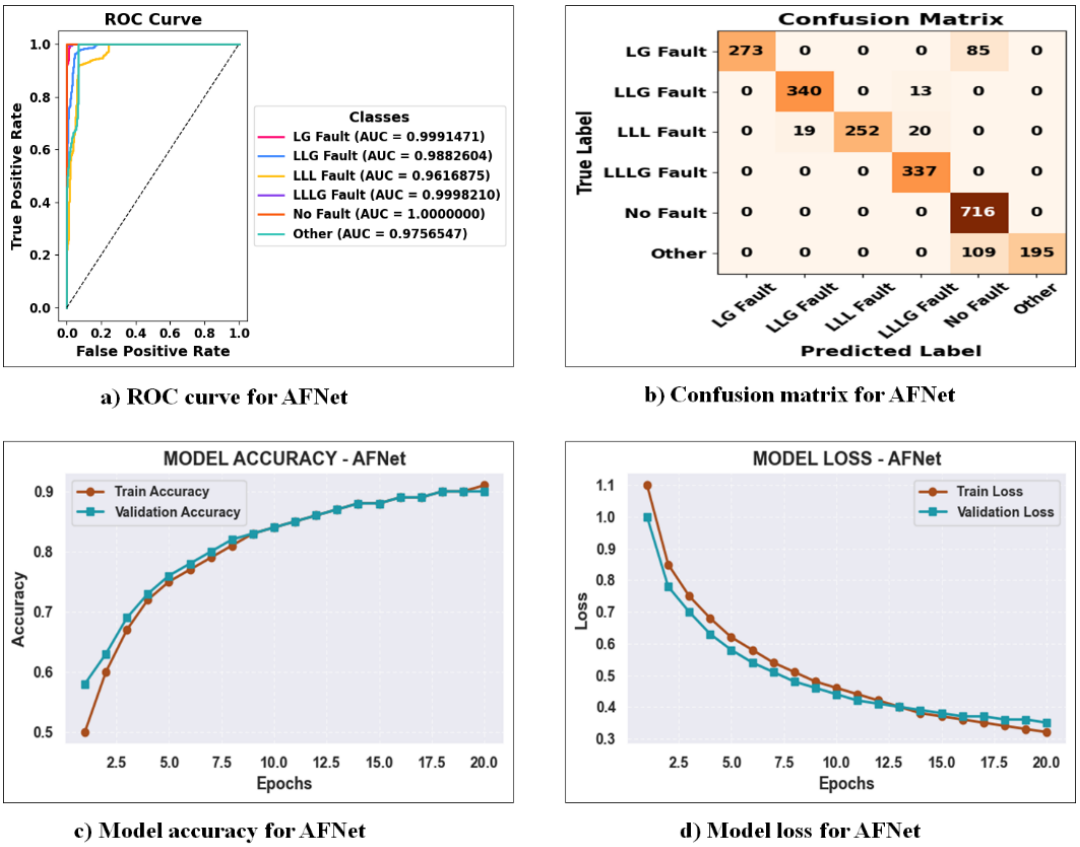

a) ROC curve for AFNet

b) Confusion matrix for AFNet

c) Model accuracy for AFNet

d) Model loss for AFNet

Fig. 10. a) ROC curve for AFNet, b) Confusion matrix for AFNet, c) Model accuracy for AFNet, d) Model loss for AFNet.

In terms of AUC values in Fig. 10, AFNet's results demonstrate the potential to achieve nearly 90% accuracy across various types of faults. However, it suffers from significant misclassification rates across several classes. Nevertheless, classification accuracy continues to increase, and training loss continues to decrease throughout the model's development and demonstrates that it sufficiently trained but less effectively than more enhanced classifiers.

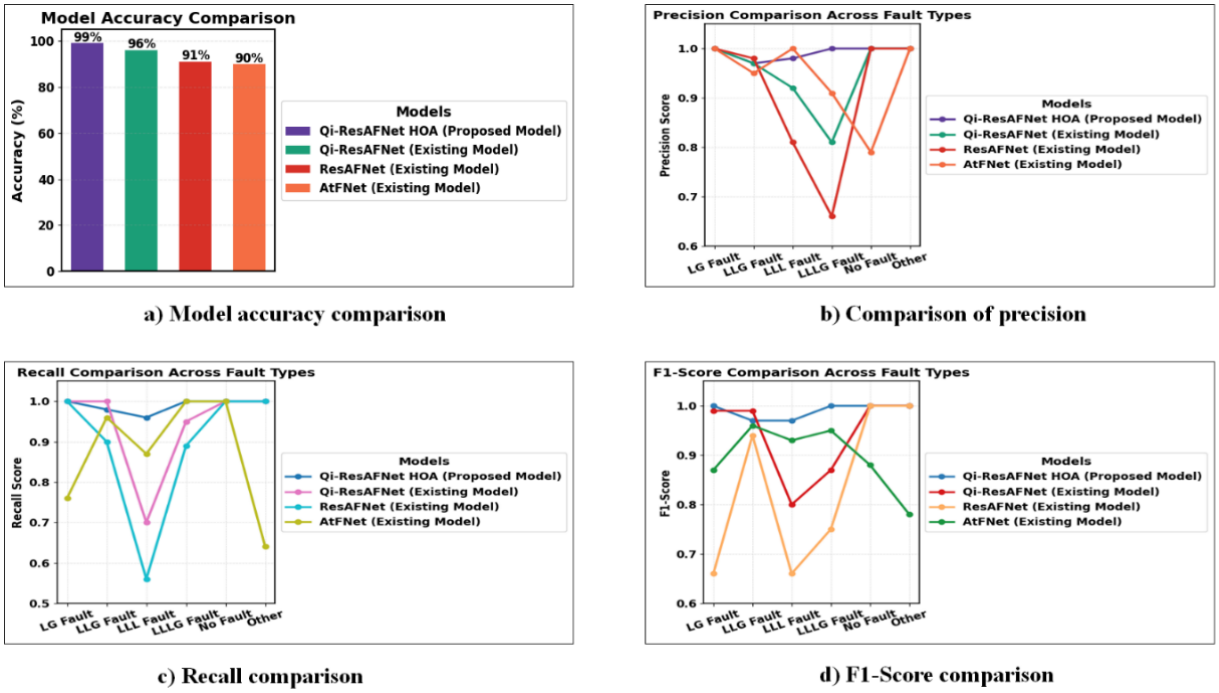

a) Model accuracy comparison

b) Comparison of precision

c) Recall comparison

d) F1-Score comparison

Fig. 11. a) Model accuracy comparison, b) Comparison of precision, c) Recall comparison, d) F1-Score comparison.

Fig. 11 clearly demonstrate that the proposed Qi-ResAFNet-HOA outperforms the Qi-ResAFNet, ResAFNet, and AFNet. The Qi-ResAFNet-HOA produces the highest accuracy and produces consistently superior levels of precision, recall, and F1-scores across each class of fault.

TABLE VIII
COMPUTATIONAL BENCHMARK

Metric	Value
Total parameters	60,038
Inference time (Total)	0.3495 s
Inference time per sample	0.2222 ms
Model size	0.81 MB
Operating system	Windows 10
Processor	Intel64 family 6 model 158 stepping 10, Genuine Intel
Tensor flow version	2.19.0
Python version	3.10
GPU availability	CPU Only (No GPU)

In table VIII, the proposed model weighs only 0.81 MB of model size and provide 60,038 parameters, enabling efficient inference of 0.2222 ms latency under specific experimental CPU; while, the actual latency for embedded or edge protection systems differ because of processor, memory and hardware specification. Further, the testing is performed on Windows 10 OS on Intel-based CPUs with Tensor Flow 2.19.0 and Python 3.10 without GPU acceleration.

TABLE IX
COMPARATIVE ANALYSIS OF ACCURACY

SI.NO	METHODS	ACCURACY
1	DT [24]	0.79
2	RF [22]	0.90
3	KNN [23]	0.93
4	LSTM-AE [26]	0.98
5	PROPOSED	0.99

According to the results of the comparison in table IX, the proposed approach is improved than all other approaches, including LSTM-AE (0.98), KNN (0.93), RF (0.90), and DT (0.79), with its accuracy score being the highest at 0.99. Hence, the proposed model provides superior results in this regard.

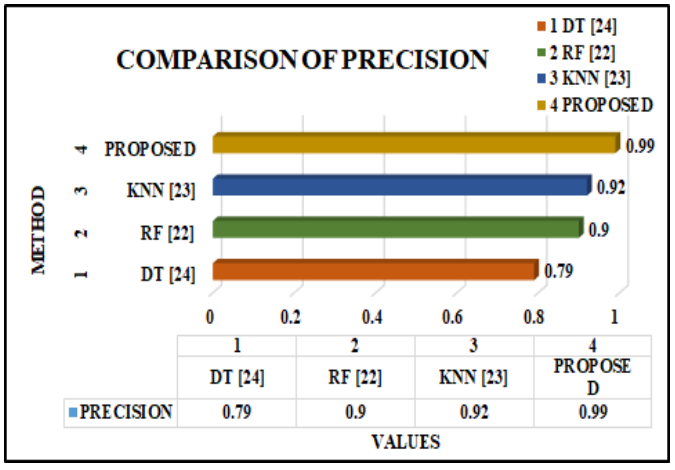

Fig. 12. Comparison of precision.

Fig. 12 illustrates that the proposed approach is superior to KNN (0.92), RF (0.90), and DT (0.79) in terms of the precision metric, with its precision being the highest at 0.99. Therefore, the proposed model is superior in providing accurate positive predictions.

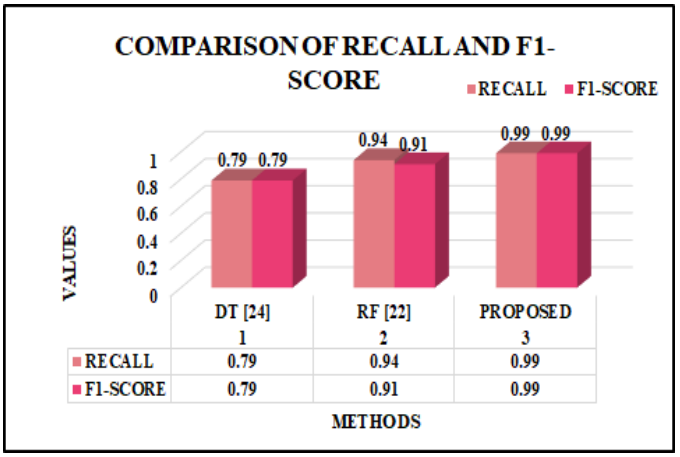

Fig. 13. Comparative analysis of recall and F1-Score.

Fig. 13 demonstrates that the proposed approach provides the highest recall and F1 score (0.99 each), followed by RF (recall 0.94, F1 score 0.91) and DT (recall 0.79, F1 score 0.79). Thus, the proposed model provides the most balanced and dependable performance classification metrics.

TABLE X
COMPARISON OF PERFORMANCE METRICS

SL NO	METHODS	ACCURACY	PRECISION	RECALL	F1-SCORE
1	DT [24]	0.790	0.793	0.792	0.792
2	RF [22]	0.9	0.9	0.94	0.91
3	PROPOSED	0.99	0.99	0.99	0.99

In table X, the proposed approach is superior to both DT and RF across all evaluation criteria such as accuracy, precision, recall and F1 score, achieves 0.99 demonstrating superior and stable results.

In order to evaluate the computational performance of the Qi-ResAFNet model adopted in the study, a number of tests are conducted on a Windows 10 environment with Intel64 Family 6 Model 158 Stepping 10 processor and TensorFlow 2.19.0 using CPU. As per testing performed, the presented model is able to complete the training in 7.81 seconds, producing an inference time of 0.3495 s and averaging an inference time of 0.2222 ms per each sample processed. In addition, the developed approach has shown 60,038 parameters to be adjusted, with the memory required of 0.81 MB.

V. CONCLUSION

The hybrid Qi-ResAFNet based fault diagnosis framework accomplished all steps of the fault diagnosis process from data acquisition through the final classification of faults, resulting in a reliable and efficient diagnostic for integrated power transmission networks. The pre-processing stage ensured dataset consistency and normalization to provide a more reliable basis for subsequent analysis. The EDA stage provides

meaningful insights into the statistical properties and relationships amongst the data, which helps the user build a better understanding of the power transmission system under fault and non-fault conditions. The feature engineering stage provides the model with strong discriminative capabilities by extracting important time-domain and frequency-domain characteristics that allow an accurate representation of the power transmission system dynamically. The classification model Qi-ResAFNet employs residual connections and attention-based fusion to enhance deep feature learning through multiple layers of feature extraction, and this results in the improved accuracy, stability and robustness of the classification results. The incorporation of the HOA provides optimal hyperparameter tuning, which results in faster convergence and improved complete performance of the classification model. Therefore, by combining these various stages of the proposed fault diagnosis framework, the proposed fault diagnosis framework demonstrated improved diagnostic accuracy, precision, recall and F1-Score of 0.99 under a variety of different conditions, thereby demonstrating the effectiveness of the proposed fault diagnosis system. While HOA is efficient in hyperparameter optimization and obtained superior classification results, this paper lacks an extensive comparison of HOA with other optimization methods. In the future, a comparative study is performed for the efficiencies of optimization methods in fault diagnosis applications.

APPENDIX

Pseudocode: Qi-ResAFNet- HOA

Input:
Dataset D = {(Xi, Yi)}
Learning rate η
Max epochs E
Population size P (for HOA)
Network parameters θ
Output:
Optimized network parameters θ*
Begin
1. Initialize Qi-ResAFNet parameters θ randomly
2. Initialize HOA population H = {h1, h2, ..., hP}
3. Evaluate initial fitness for each hi
4. For epoch = 1 to E do
For each mini-batch (X, Y) in D do
Forward Pass
4.1 F1 = Convolution_Block (X)
4.2 F2 = Residual_Block (F1)
4.3 F3 = Quantum_Encoding (F2)
4.4 F4 = Attention_Fusion (F3)
4.5 Ŷ = Fully_Connected (F4)
Loss Computation
4.6 L = Cross Entropy(Y, Ŷ)
Back propagation
4.7 Compute gradients ∇θ L
4.8 Update θ using HOA optimizer
End For
4.9 Evaluate validation accuracy
End For
5. Return optimized parameters θ
End

Function Quantum_Residual_Attention_Fusion (Input Feature F)
1. Apply Quantum Phase Encoding:
QF = |ψ> = α|0> + β|1> transformation of F
2. Residual Learning:
R = F + Conv (F)
3. Channel Attention:
CA = Sigmoid(FC(GlobalAvgPool (R)))
R1 = R ⊗ CA
4. Spatial Attention:
SA = Sigmoid (Conv(R1))
R2 = R1 ⊗ SA
5. Fusion:
Output = Concatenate(QF, R2)
Return Output
End Function

Input:
Population H = {h1, h2, ..., hP}
Fitness function f()
Max iterations T
Output:
Best solution h*
Begin
1. Initialize population randomly
2. Evaluate fitness f(hi)
3. For t = 1 to T do
3.1 Identify best heron h_{best}
3.2 For each heron hi do
Exploration phase
hi_new = hi + r1*(h_{best} - |hi|)
Exploitation phase
hi_{new}= hi_{new}+ r2*(mean(H) - hi)
Evaluate fitness f(hi_{new})
If f(hi_{new}) better than f(hi)
Replace hi with hi_{new}
End If
End For
End For
4. Return h_{best}

END

ACKNOWLEDGMENT

Not Applicable

REFERENCES

[1] J. Feng, T. Yu, K. Zhang, and L. Cheng, "Integration of multi-agent systems and artificial intelligence in self-healing subway power supply systems: Advancements in fault diagnosis, isolation, and recovery," *Processes*, vol. 13, no. 4, pp. 1144, Apr. 2025. https://doi.org/10.3390/pr13041144.

[2] M. Kouraichi, M. Mansouri, M. Trabelsi, A. M'Halla, A. S. Abdel-Khalik, and A. Sakly, "Deep learning for fault diagnosis in power transmission lines: Current trends, limitations, and future directions," *IEEE Access*, vol. 13, pp. 192105-192142, Nov. 2025. https://doi.org/10.1109/ACCESS.2025.3628908.

[3] R. Xu, and J. Zhang, "Intelligent information systems for power grid fault analysis by computer communication technology," *Energy Informatics*,

vol. 8, no. 1, pp. 10, Jan. 2025. https://doi.org/10.1186/s42162-024-00465-6.
[4] M. Talaat, M. H. Elkholy, A. Alblawi, and T. Said, "Artificial intelligence applications for microgrids integration and management of hybrid renewable energy sources," *Artificial Intelligence Review*, vol. 56, no. 9, pp. 10557-10611, Sep. 2023. https://doi.org/10.1007/s10462-023-10410-w.
[5] J. Zhang, K. Zhang, Y. An, H. Luo, and S. Yin, "An integrated multitasking intelligent bearing fault diagnosis scheme based on representation learning under imbalanced sample condition," *IEEE Transactions on Neural Networks and Learning Systems*, vol. 35, no. 5, pp. 6231-6242, Jan. 2023. https://doi.org/10.1109/TNNLS.2022.3232147.
[6] S. Gadu, G. Himaja, D. H. A. Reddy, M. D. P. Sai, and B. T. Prashant, "An era: Review on emerging technologies for AR/VR/MR," *In AIP Conference Proceedings*, vol. 3306, no. 1, pp. 050002. AIP Publishing LLC, Jun. 2025. https://doi.org/10.1063/5.0276251.
[7] Z. Li, Y. Zhang, H. Wu, S. Suzuki, A. Namiki, and W. Wang, "Design and application of a UAV autonomous inspection system for high-voltage power transmission lines," *Remote Sensing*, vol. 15, no. 3, pp. 865, Feb. 2023. https://doi.org/10.3390/rs15030865.
[8] P. Arévalo, and F. Jurado, "Impact of artificial intelligence on the planning and operation of distributed energy systems in smart grids," *Energies*, vol. 17, no. 17, pp. 4501, Sep. 2024. https://doi.org/10.3390/en17174501.
[9] B. L. Nguyen, T. V. Vu, T. T. Nguyen, M. Panwar, and R. Hovsapian, "Spatial-temporal recurrent graph neural networks for fault diagnostics in power distribution systems," *IEEE Access*, vol. 11, pp. 46039-46050, May 2023. https://doi.org/10.1109/ACCESS.2023.3273292.
[10] R. Sivakumar, "Investigation of Casting Quality Control Through Deep Learning Techniques," *2025 8th International Conference on Trends in Electronics and Informatics (ICOEI), Tirunelveli, India*, pp. 1-5, Apr. 2025. https://doi.org/10.1109/ICOEI65986.2025.11013536.
[11] C. He, H. Shi, J. Si, and J. Li, "Physics-informed interpretable wavelet weight initialization and balanced dynamic adaptive threshold for intelligent fault diagnosis of rolling bearings," *Journal of Manufacturing Systems*, vol. 70, pp. 579-592, Oct. 2023. https://doi.org/10.1016/j.jmsy.2023.08.014.
[12] K. Karthika, and D. P. Rangasamy, "Authorization of Aadhar data using Diffie Helman key with enhanced security concerns," *Journal of Intelligent & Fuzzy Systems*, Apr. 2024. https://doi.org/10.3233/JIFS-234641.
[13] S. Yan, H. Shao, J. Wang, X. Zheng, and B. Liu, "LiConvFormer: A lightweight fault diagnosis framework using separable multiscale convolution and broadcast self-attention," *Expert Systems with Applications*, vol. 237, pp. 121338, Mar. 2024. https://doi.org/10.1016/j.eswa.2023.121338.
[14] M. Kiasari, M. Ghaffari, and H. H. Aly, "A comprehensive review of the current status of smart grid technologies for renewable energies integration and future trends: The role of machine learning and energy storage systems," *Energies*, vol. 17, no. 16, pp. 4128, Aug. 2024. https://doi.org/10.3390/en17164128.
[15] K. Zhou, E. Diehl, and J. Tang, "Deep convolutional generative adversarial network with semi-supervised learning enabled physics elucidation for extended gear fault diagnosis under data limitations," *Mechanical Systems and Signal Processing*, vol. 185, pp. 109772, Feb. 2023. https://doi.org/10.1016/j.ymssp.2022.109772.
[16] A. Al Mamun, M. M. Bappy, A. S. Mudiyanselage, J. Li, Z. Jiang, Z. Tian, S. Fuller, T. C. Falls, L. Bian, and W. Tian, "Multi-channel sensor fusion for real-time bearing fault diagnosis by frequency-domain multilinear principal component analysis," *The International Journal of Advanced Manufacturing Technology*, vol. 124, no. 3, pp. 1321-1334, Jan. 2023, https://doi.org/10.1007/s00170-022-10525-4.
[17] V. Varriale, A. Cammarano, F. Michelino, and M. Caputo, "Critical analysis of the impact of artificial intelligence integration with cutting-edge technologies for production systems," *Journal of Intelligent Manufacturing*, vol. 36, no. 1, pp. 61-93, Jan. 2025. https://doi.org/10.1007/s10845-023-02244-8.
[18] E. B. Weiner, I. Dankwa-Mullan, W. A. Nelson, and S. Hassanpour, "Ethical challenges and evolving strategies in the integration of artificial intelligence into clinical practice," *PLOS digital health*, vol. 4, no. 4, pp. e0000810, Apr. 2025. https://doi.org/10.1371/journal.pdig.0000810.
[19] J. Wang, H. Shao, S. Yan, and B. Liu, "C-ECAFormer: A new lightweight fault diagnosis framework towards heavy noise and small samples," *Engineering Applications of Artificial Intelligence*, vol. 126, pp. 107031, Nov. 2023. https://doi.org/10.1016/j.engappai.2023.107031.
[20] K. Kumar, S. V. Pande, T. C. A. Kumar, P. Saini, A. Chaturvedi, P. C. S. Reddy, and K. B. Shah, "Intelligent controller design and fault prediction using machine learning model," *International Transactions on Electrical Energy Systems*, vol. 2023, no. 1, pp. 1056387, 2023. https://doi.org/10.1155/2023/1056387.
[21] P. Sun, X. Liu, M. Lin, J. Wang, T. Jiang, and Y. Wang, "Transmission line fault diagnosis method based on improved multiple SVM model," *IEEE Access*, vol. 11, pp. 133825-133834, Nov. 2023. https://doi.org/10.1109/ACCESS.2023.3333939.
[22] C. Li, and B. Wang, "A knowledge graph method towards power system fault diagnosis and classification," *Electronics*, vol. 12, no. 23, pp. 4808, Nov. 2023. https://doi.org/10.3390/electronics12234808.
[23] N. K. Abed, F. T. Abed, H. F. Al-Yasriy, and H. S. Alrikabi, "Detection of power transmission lines faults based on voltages and currents values using K-nearest neighbors," *International Journal of Power Electronics and Drive Systems (IJPEDS)*, vol. 14, no. 02, pp. 1033-1043, Jun. 2023. 10.11591/ijpeds.v14.i2.pp1033-1043.
[24] H. N. Noura, Z. Allal, O. Salman, and K. Chahine, "Feature engineering for fault detection and diagnosis in power transmission lines using a tree-based approach," *e-Prime-Advances in Electrical Engineering, Electronics and Energy*, vol. 12, pp. 100991, Jun. 2025. https://doi.org/10.1016/j.prime.2025.100991.
[25] R. Nawaz, A. Wadood, K. K. Mehmood, S. B. A. Bukhari, H. Albalawi, A. M. Alatwi, and M. Sajid, "Gradient boosting feature selection for integrated fault diagnosis in series-compensated transmission lines," *IEEE Access*, Apr. 2025. https://doi.org/10.1109/ACCESS.2025.3558796.
[26] M.D. Hossain, "Adaptive fault diagnosis in power transmission lines using deep learning and LSTM autoencoders for enhancing grid reliability." International Journal of Electrical Power & Energy Systems 174 (2026): 111458.

Dr. Sanepalle Gopal Reddy Graduated from JNTU, Hyderabad in 2001. He had completed his M. Tech in Energy Systems from VTU Belgaum, Karnataka in 2003. He completed Ph. D from Annamalai University, Tamil Nadu in 2025. He is working as an Associate Professor in EEE at Jyothishmathi Institute of Technology and Science, Karimnagar, Telangana-505527. He published 10 research papers in national, international journals and conferences. His areas of interest are Electro Magnetic Fields, High Voltage Engineering, Renewable energy sources and Power Systems.

Dr. Athimamula Srujana Graduated from Kakatiya Institute of Technology and Science, Warangal in 1998. She had completed M. Tech in Power Electronics from JNTU, Hyderabad in 2002. She completed Ph. D from JNTU, Hyderabad in 2011. She is working as a Principal and Professor at Vidya Jyothi Institute of Technology (VJIT), Hyderabad, Telangana. She published 40 research papers in national, international journals and conferences. Her areas of interest are Power Electronics and Power Systems.

Dr. N. Narender Reddy was born in Kodad, India, in 1984. He is presently working as Associate Professor in Degree Engineering Department, Military College of Electronics and Mechanical Engineering, Secunderabad, Telangana State, India – 500015. Previously he was worked in Sri Venkateswara Engineering College Suryapet. He received his Ph.D from K L University Vijayawada in November 2022, M.Tech from JNTU Hyderabad in 2011 and B.Tech from JNTU Hyderabad in 2006 and he has more than eighteen years of teaching experience. He published one text book in the field of Power Electronics. He published 28 research papers in reputated National and International journals and participated in 6 National and International conferences. He also had two patent publications. His research area includes Electric Vehicles, Power Quality, Microgrids, Predictive Controllers, Kalaman Filters and Particle Swarm Optimization.

Dr. K. Shashidhar Reddy Graduated from JNTU, Hyderabad in 2001. He had completed his M. Tech in Energy Systems from VTU Belagaum, Karnataka in 2003. He completed Ph.D from JNTUH, Hyderabad Telangana in 2015. He is working as a Professor in CVR College of Engineering, Hyderabad- 501510. He published 40 research papers in national, international journals and conferences. His areas of interest are Power Transformers, High Voltage Engineering, Renewable energy sources and Power Systems.